scientific reports

Check for updates

OPEN

Siglec6 CAR T cells suppressed progression of AML via inhibiting Siglec6 and SHP2 induced Src and ERK signaling activation

Qian Li[1,2], Li Lin[2], Shuang Gao[2], Lin Chen[2], Zhiying Zhang[2], Jing Ma[2], Su Liu[2], Zeng Cao[1], Haifeng Zhao[1]✉ & Yafei Wang[1,2]✉

To explore the specific molecular mechanisms of Siglec6 CAR-T therapy in acute myeloid leukemia (AML). AML samples were selected from the GEO database for bioinformatics analysis. Siglec6 was knocked down and overexpressed in MOLM-13 cells through lentiviral infection, and then injected into NOD/SCID mice via the tail vein to detect the distribution of AML in mice using in vivo imaging. MOLM-13 cells were divided into six groups: oe-NC, oe-Siglec6, oe-Siglec6 + PHPS1, oe-Siglec6 + Dasatinib, oe-Siglec6 + Dasatinib + Lovastatin, and oe-Siglec6 + Dasatinib + Lovastatin + IL-3 neutralizing antibody. The expression levels of related proteins were detected by Western blot and immunofluorescence, and the cell invasion and proliferation abilities were tested by Transwell and CCK8 assays. Finally, MOLM-13 cells were co-cultured with CD19-CAR-T and Siglec6-CAR-T cells, and the apoptosis level of MOLM-13 cells after co-culture was detected by flow cytometry. In vivo imaging found that after overexpression of Siglec6 in MOLM-13 cells, AML cells were more widely distributed in mice; Western blot and immunofluorescence detected the protein levels in AML cells and found that compared with the oe-NC group, the expression levels of Siglec6, p-SHP2, IL-3, and p-ERK1/2 proteins were increased in the oe-Siglec6 group; cell invasion, migration, and proliferation abilities were enhanced, and these abilities were reversed after treatment with SHP2 inhibitors, Src inhibitors, SHP2 agonists, and IL-3 neutralizing antibodies. Finally, both in vitro and in vivo, it was found that compared with CD19 CAR-T, the apoptosis level of AML cells treated with Siglec6 CAR-T was increased, and their distribution in mice was reduced. Siglec6 CAR-T reduces the proliferation, invasion, and migration abilities of AML cells by acting on the SHP2/Src/ERK/IL-3 axis.

Keywords CAR-T, AML, Siglec6, SHP2, Src, IL-3, ERK

Acute myeloid leukemia (AML) is the most common type of acute leukemia in adults. It is characterized by the malignant transformation and uncontrolled proliferation of myeloid hematopoietic progenitor cells, leading to the accumulation of a large number of immature cells in the bone marrow and peripheral blood. Standard induction chemotherapy can achieve a complete remission rate of 60–80% in AML. However, ultimately, 50–70% of AML patients still relapse, and the 5-year survival rate is only 20–30%[1,2]. Chemotherapy resistance and short-term relapse remain the main factors threatening patient survival[3]. Although the survival of acute leukemia has been extended with the application of hematopoietic stem cell transplantation and small molecule inhibitors, the 5-year survival rate of AML patients after treatment is still low due to the high relapse rate of AML. Therefore, there is an urgent need for a new treatment method for AML[4].

In recent years, CAR T-cell (CAR-T) technology has attracted widespread attention in the treatment of AML. Some specific antigens expressed on the surface of AML cells, such as CD19, CD33, CD123, etc., provide the possibility for precise recognition and targeted treatment of CAR-T cells[5]. Through the design of chimeric antigen receptors, CAR-T cells can effectively activate T cells, recognize and kill AML cells, thereby theoretically achieving targeted treatment of the disease[6]. However, although CAR-T cell therapy has achieved significant efficacy in some hematological malignancies, its application in AML has not been ideal, often facing low cure

[1]Department of Hematology, Tianjin Key Laboratory of Cancer Prevention and Therapy, Tianjin Medical University Cancer Institute and Hospital, National Clinical Research Center of Cancer, Tianjin's Clinical Research Center for Cancer, Tianjin, China. [2]Department of Blood and Marrow Transplantation, Tianjin Cancer Hospital Airport Hospital, Tianjin, China. ✉email: hzhao02@tmu.edu.cn; yfwang@tmu.edu.cn

rates and high relapse risks[7]. This is mainly related to the heterogeneity of AML cells and their adaptive changes to treatment. At the same time, the expression of antigens on the surface of AML cells also has certain variability, which limits the recognition and killing of target cells by CAR-T cells. Therefore, to improve the effectiveness of CAR-T cells in the treatment of AML, it is urgent to explore the possibility of targeting other AML-specific antigens.

Siglec-6 (sialic acid-binding immunoglobulin-like lectin-6) is an immunomodulatory cell surface receptor belonging to the Siglec family[8]. It consists of three extracellular immunoglobulin (Ig) domains and two intracellular immunoreceptor tyrosine-based inhibitory motifs (ITIMs), and its molecular structure is very similar to that of Siglec-3 (CD33)[9]. Siglec-6 is expressed in AML, but not detected in normal hematopoietic stem cells and progenitor cells[10]. This allows CAR-T cells to accurately recognize and kill AML cells by targeting Siglec6 on AML, demonstrating enormous clinical potential[11]. Therefore, we have conducted in-depth research on the Siglec-6 target in AML in order to seek more effective treatment strategies.

SHP2 is an important tyrosine phosphatase encoded by the *PTPN11* gene and is a key regulatory factor in cellular signal transduction pathways[12]. SHP2 plays a crucial role in various cellular processes, including cell proliferation, differentiation, and survival. This protein contains two SH2 domains that can specifically bind to phosphorylated tyrosine residues, thereby transmitting signals within cells. The main function of SHP2 is dephosphorylation, which can regulate various intracellular signaling pathways, such as cell growth factor receptors, integrins, and immune receptor signaling pathways. By removing tyrosine phosphate groups, SHP2 plays a negative regulatory role, promoting the termination or regulation of downstream signals. It has also been shown that there is a direct interaction between Siglec6 and SHP2. Siglec6 inhibits downstream signaling pathways, such as Src, IL-3, and ERK signaling pathways, by recruiting SHP2. This interaction is critical for understanding the mechanism of Siglec6 CAR T cells. Previous studies may have reported aberrant expression or function of SHP2 in AML. Therefore, we speculate that SHP2 plays a key role in AML, and its abnormal expression or activation is closely related to the development of AML. In-depth exploration of the molecular mechanisms affecting SHP2 expression levels in AML may provide new strategies for the treatment of AML.

Materials and methods

Preparation of CAR-T cells

First, we prepared the CAR component of CAR-T cells. Siglec6-CAR consists of a CD8α signal peptide, a human anti-Siglec6 scFv, a CD8α hinge, a CD8α transmembrane, a 4-1BB intracellular co-stimulatory domain, and an intracellular CD3ζ domain. The control CD19-CAR is composed of a CD8α signal peptide, a human anti-CD19 scFv, a CD8α hinge, a CD8α transmembrane, a 4-1BB intracellular co-stimulatory domain, and an intracellular CD3ζ domain. Polyethyleneimine (PEI) was used to co-transfect HEK-293T with CAR vectors and two packaging plasmids (pMD.2G and psPAX2). After transfection, the supernatant was collected at 48 and 72 h, filtered through a 0.45 μm filter (Millipore), and then centrifuged at 100,000×g for 120 min at 4 °C. The concentrated virus was resuspended and stored at − 80 °C. Lentivirus titration was performed using the TCID50 method.

For T cell preparation, we purchased peripheral blood mononuclear cells (PBMCs) from Hunan Fenghui Bio, purified them by Ficoll-Paque PLUS (GE Healthcare) density gradient, and stored them frozen. On the day before CAR-T cell production, PBMCs were thawed at 37 °C and incubated overnight in RPMI 1640 with 10% FBS, penicillin, streptomycin, amphotericin B, and L-glutamine at 37 °C and 5% CO2. The next day, PBMCs were activated with a 1:1 ratio of CD3:CD28 beads (Invitrogen) for 40 to 48 h. Subsequently, the CAR construct was transferred into activated T cells through lentiviral infection to produce CD19-CAR-T and Siglec6-CAR-T.

AML cell culture, infection, and treatment

MOLM-13 cells, purchased from Procell, were cultured in RPMI1640 medium (11875093, Thermo Fisher) containing 10% fetal bovine serum (A5256701, Thermo Fisher). The cells were authenticated by Short Tandem Repeat (STR) and confirmed to be free of contamination. They were routinely cultured in a 37 °C, 5% CO2 incubator. Cells were passaged every 2–3 days, and cells in the logarithmic growth phase were used for subsequent experiments. To infect MOLM-13 cells with lentivirus, they were seeded into 24-well plates the day before infection and grown to 50% confluence. The cells were then transduced with lentiviral vectors at a multiplicity of infection (MOI) of 10 using lentivirus oe-Siglec6 (2 × 10^9 TU/ml) and sh-Siglec6 (2 × 10^9 TU/ml) from Yunzhou Bio, with a control vector for comparison. After 48 h, cells were selected with puromycin (2 μg/mL) for two weeks.

A portion of MOLM-13 cells were treated with 10 μg/mL of SHP2 inhibitor (PHPS1, MCE), 10 μg/mL of Src inhibitor (S1021, Selleck), and 5 μg/mL SHP2 agonist (75330-75-5, Merck) for 12 h to promote and inhibit protein expression levels. Another portion of MOLM-13 cells were co-cultured with CAR-T cells at a 1:3 ratio to investigate the killing effect of CAR-modified T cells on AML cells.

Animal modeling and in vivo imaging

Two-week-old, 16–18 g NOD/SCID mice, purchased from Vital River, were bred under specific pathogen-free conditions. Nude mice were randomly divided into five groups: oe-NC, oe-NC + CAR-T, oe-Siglec6, oe-Siglec6 + CAR-T, and oe-Siglec6 + Siglec6 CAR-T, with six mice per group. Luc-labeled MOLM-13 AML cells in the logarithmic growth phase were centrifuged, counted, and adjusted to a cell density of 1 × 10^7/mL with PBS. MOLM-13 cells were injected into mice via the tail vein. Tumor implantation was confirmed 25 days later. Subsequently, treated CD19-CAR-T and Siglec6-CAR-T cells were injected into the mice, and disease progression was monitored and tumor volume measured using bioluminescence imaging on day 28. Mice were anesthetized with 2% isoflurane in a nose cone and maintained under inhalation anesthesia. D-luciferin (Goldbio, 150 mg/kg) was administered intraperitoneally 10 min before scanning. After the experiment, mice were euthanized

by CO2 inhalation. All experimental protocols were approved by the Ethics Committee of Tianjin Jinke Bona Biotechnology Co. A statement that all methods have been performed in accordance with relevant guidelines and regulations and are reported in accordance with ARRIVE guidelines.

Western blot

Collected MOLM-13 cells that had been treated with lentiviral infection and protein agonists and antagonists, as well as IL-3 monoclonal antibody, were lysed with RIPA lysis buffer (P0013B, Beyotime) containing the protease inhibitor PMSF (ST506, Beyotime) to extract total protein. Protein quantification was performed using the BCA assay kit. Proteins were separated by SDS-PAGE electrophoresis, transferred to PVDF membranes. At room temperature and closed with 5% skimmed milk for 2 h. The membranes were then incubated with primary antibodies against Siglec6 (1:1000, abcam), p-SHP2 (1:500, abclonal), IL-3 (1:1000, abcam), p-ERK1/2 (1:500, Thermofisher), MMP2 (1:1000, abcam), MMP9 (1:500, abclonal), CyclinA1 (1:2000, Thermofisher), CyclinD1 (1:1000, abclonal), Ki-67 (1:1000, abcam), cleaved-Caspase-3 (1:1000, abcam), cleaved-Caspase-9 (1:1000, abcam) and GAPDH (1:2000, abcam). HRP-conjugated goat anti-rabbit and goat anti-mouse secondary antibodies (1:5000, abcam) were added and incubated for 1 h at room temperature. The membranes were washed with TBST, and ECL chemiluminescence reagent was used for development. Quantitative analysis was performed using Image J software.

Immunofluorescence

Cell culture medium was removed, and cells were fixed with 4% paraformaldehyde at room temperature for 20 min. After washing with phosphate buffer saline (PBS), cells were permeabilized with PBS containing 0.1% Triton X100 for 5 min, followed by blocking with 10% skim milk for 1 h to block non-specific antibody binding sites. Cells were then incubated overnight at 4 °C with Siglec6 (1:1000, abcam) and p-SHP2 (1:100, abcam) antibodies. After washing three times with PBS, goat anti-rabbit and donkey anti-mouse secondary antibodies were added and incubated for 1 h at room temperature. Finally, DAPI was used to counterstain the cell nuclei. DAPI was diluted to a concentration of 1 μg/mL with PBS. The diluted DAPI was added and incubated for 10 min at room temperature. Cells were washed 3 times with PBS for 5 min each to remove unbound DAPI. Images were visualized using an inverted fluorescence microscope (OLYMPUS, IX73) and quantified using imageJ.

CCK8 analysis

MOLM-13 cells were collected after 12, 24, and 48 h of treatment. The culture medium was removed from the wells, and 10μL of CCK-8 solution was added to each well. The plates were incubated for 2 h at 37 °C and 5% CO2. Absorbance (A) values at 450 nm were measured using a microplate reader.

Transwell invasion assay

MOLM-13 cells were seeded at a density of 5 × 10^4/mL in the upper chamber of a Transwell plate pre-coated with Matrigel. 600 μL of culture medium containing 20% fetal bovine serum was added to the lower chamber. After 24 h, the lower chamber was washed twice with PBS, and cells were fixed with 4% paraformaldehyde for 30 min and stained with 0.1% crystal violet solution for 20 min. Quantitative analysis was performed using Image J software in six random fields of view.

Flow cytometry for apoptosis

CAR-T and MOLM-13 cells were separated using Ficoll-Paque. The MOLM-13 cell suspension was centrifuged for 5 min and washed three times with PBS. Cells were stained with 500 μl of binding buffer and gently mixed, followed by the addition of 5 μl of PI and 5 μl of Annexin V (C1062S, Beyotime) and thorough mixing. Cells were incubated at room temperature for 15 min. Apoptosis levels were detected by flow cytometry after 1 h and quantified using FlowJo software (version FlowJo v10.9, https://www.flowjo.com/). The experiments were repeated three times.

Bioinformatics analysis of AML

Downloaded datasets related to acute myeloid leukemia, GSE10358 and GSE24395, from the Gene Expression Omnibus database (https://www.ncbi.nlm.nih.gov/geo/). First, background correction and normalization were performed using the Robust Multi-array Average (RMA) (version 1.70.0, https://bioconductor.org/packages/release/bioc/html/affy.html) method, which is a standard step in processing microarray data. RMA not only effectively removes background noise but also enhances the comparability of data across different chips. Next, the Combat (version 3.40.0, https://bioconductor.org/packages/release/bioc/html/sva.html) method was applied for batch effect correction, which can eliminate technical variations between different experimental batches, ensuring the accuracy of subsequent analyses. In the differential expression analysis, the limma package (version 3.46.0, https://bioconductor.org/packages/release/bioc/html/limma.html) was utilized to efficiently identify genes with significant expression differences under different conditions. The selection criteria were set to |log2 Fold Change|>1 and p-value < 0.05, ensuring that the selected genes are biologically significant. Further multiple hypothesis testing was corrected using the Benjamini-Hochberg method to control the false positive rate. By using the ggplot2 package (version 3.3.5, https://ggplot2.tidyverse.org) for visualizing the results of the differential analysis, the expression patterns of significantly different genes can be intuitively displayed. This visualization not only aids in the interpretation of results but also provides a foundation for subsequent biological analyses. Among the identified differentially expressed genes, the ClusterProfiler package (version 3.18.1, https://bioconductor.org/packages/release/bioc/html/clusterProfiler.html) was used for GO and KEGG pathway enrichment analysis, revealing the roles of these genes in cellular components, molecular functions, and biological processes. Additionally, KEGG pathway analysis helps to understand the role of these genes in

key biological pathways, thereby providing clues for potential treatment strategies for AML. Finally, by selecting the Spearman statistical method, a correlation analysis (R version 4.1.0, https://www.r-project.org) of differential genes was performed to discover potential associations between gene variables.

Statistical analysis

Statistical analysis was performed using GraphPad Prism 8.0.2. Statistical significance was assessed using analysis of variance (ANOVA) or t-tests, with Tukey's post-hoc test. A P-value of less than 0.05 was considered statistically significant. All results are expressed as the mean ± standard error of the mean (SEM). Cellular experiments were independently repeated three times, and animal experiments were conducted with six animals per group.

Results

1. Bioinformatics Analysis of AML.

Through analysis with the limma package, a total of 397 significantly differentially expressed genes (DEGs) were identified in the GSE10358 dataset, with 238 upregulated and 159 downregulated genes; the GSE24395 dataset had a total of 647 DEGs, with 415 upregulated and 232 downregulated genes. The upregulation and downregulation of these genes indicate significant transcriptional changes in AML cells (Fig. 1A). Intersection analysis revealed 52 common genes (Fig. 1B). These common genes were further analyzed using GO and KEGG analyses, which showed significant enrichment results suggesting that these DEGs play important roles in cellular components, molecular functions, and biological processes. For instance, DEGs were enriched in cellular components related to the cell membrane, potentially associated with cell signaling and cell-cell interactions. Additionally, the enrichment results of molecular functions indicated that these genes may be involved in important biological functions such as enzymatic activity and binding activity, highlighting their key roles in cellular metabolism and proliferation (Fig. 1C). KEGG pathway analysis results indicated that DEGs were significantly enriched in the MAPK signaling pathway, PI3K-Akt signaling pathway, and Ras signaling pathway, which are closely related to tumor cell growth, apoptosis, and migration (Fig. 1D). Particularly, the MAPK signaling pathway is a key regulatory pathway in many types of cancer, and its activation is often associated with tumor invasiveness and drug resistance. Spearman correlation analysis revealed a positive correlation between Src and SHP2 (PTPN11), suggesting a potential synergistic role of these two in signal transduction (Fig. 1E). The positive correlation between SHP2 (PTPN11) and ERK1/2 (MAPK1) further supports the importance of the MAPK pathway in AML (Fig. 1F). The positive correlation between IL-3 and Siglec6 may reveal a potential role of IL-3 in AML cell proliferation, and Siglec6, as an immunomodulatory molecule, its expression may affect the microenvironment of AML (Fig. 1G).

2. In Vivo Experiments Demonstrate that High Expression of Siglec-6 Promotes the Distribution and Content Level of AML.

MOLM-13 cells infected with lentivirus were injected into NOD/SCID mice via the tail vein, divided into oe-NC, oe-Siglec6, sh-NC, sh-Siglec6 four groups, and the distribution of AML in mice was detected by in vivo imaging. It was found that compared with the oe-NC group, the AML content in the oe-Siglec6 group was higher and more widely distributed; compared with the sh-NC group, the AML content and distribution in the sh-Siglec6 group were both weakened (Fig. 2A, B).

3. Siglec6 Acts on AML through the SHP2/Src/ERK/IL-3 Axis.

MOLM-13 cells were divided into six groups: oe-NC, oe-Siglec6, oe-Siglec6 + PHPS1, oe-Siglec6 + Dasatinib, oe-Siglec6 + Dasatinib + Lovastatin, and oe-Siglec6 + Dasatinib + Lovastatin + IL-3 monoclonal antibody. Western blot was used to detect the protein expression levels of Siglec6, p-SHP2, IL-3, pERK1/2, and immunofluorescence was used to detect the fluorescence levels of Siglec6 and p-SHP2. It was found that compared with the oe-NC group, the protein expression levels of Siglec6, p-SHP2, IL-3, pERK1/2, and the fluorescence levels of Siglec6 and p-SHP2 in the oe-Siglec6 group were increased; compared with the oe-Siglec6 group, the protein expression levels of Siglec6, p-SHP2, IL-3, pERK1/2, and the fluorescence levels of Siglec6 and p-SHP2 in the oe-Siglec6 + PHPS1 group were weakened, and the same was true for the oe-Siglec6 + Dasatinib group; compared with the oe-Siglec6 + Dasatinib group, the protein expression levels of Siglec6, p-SHP2, IL-3, pERK1/2, and the fluorescence levels of Siglec6 and p-SHP2 in the oe-Siglec6 + Dasatinib + Lovastatin group were enhanced; while compared with the oe-Siglec6 + Dasatinib + Lovastatin group, the protein expression level of p-SHP2 and the fluorescence level of p-SHP2 in the oe-Siglec6 + Dasatinib + Lovastatin + IL-3 monoclonal antibody group remained unchanged, the protein expression levels of Siglec6, IL-3, pERK1/2 were weakened, and the fluorescence level of Siglec6 was weakened (Fig. 3A, B). This proves that Siglec6 acts on AML through the SHP2/Src/ERK/IL-3 axis.

4. Siglec6 Promotes the Proliferation and Invasion-Metastasis Abilities of AML through the SHP2/Src/ERK/IL-3 Axis.

MOLM-13 cells were divided into six groups: oe-NC, oe-Siglec6, oe-Siglec6 + PHPS1, oe-Siglec6 + Dasatinib, oe-Siglec6 + Dasatinib + Lovastatin, and oe-Siglec6 + Dasatinib + Lovastatin + IL-3 monoclonal antibody. Western blot was used to detect the expression levels of invasion-related proteins MMP2 and MMP9, and proliferation-related proteins CyclinA1, CyclinD1 and Ki-67. Transwell assays were used to test cell migration ability, and CCK8 assays were used to test cell activity. It was found that compared with the oe-NC group, the oe-Siglec6 group showed increased expression levels of MMP2, MMP9, CyclinA1, CyclinD1 and Ki-67 proteins, cell migration ability, and cell activity. Compared with the oe-Siglec6 group, the oe-Siglec6 + PHPS1 group showed decreased expression levels of MMP2, MMP9, CyclinA1, CyclinD1 and Ki-67 proteins, cell migration ability, and cell activity. Similarly, the oe-Siglec6 + Dasatinib group also showed decreased levels of these proteins, cell migration ability, and cell activity. Compared with the oe-Siglec6 + Dasatinib group, the oe-Siglec6 + Dasatinib + Lovastatin group showed increased expression levels of MMP2, MMP9, CyclinA1, CyclinD1 and Ki-67 proteins, cell migration ability, and cell activity. In contrast, compared with the oe-Siglec6 + Dasatinib + Lovastatin group,

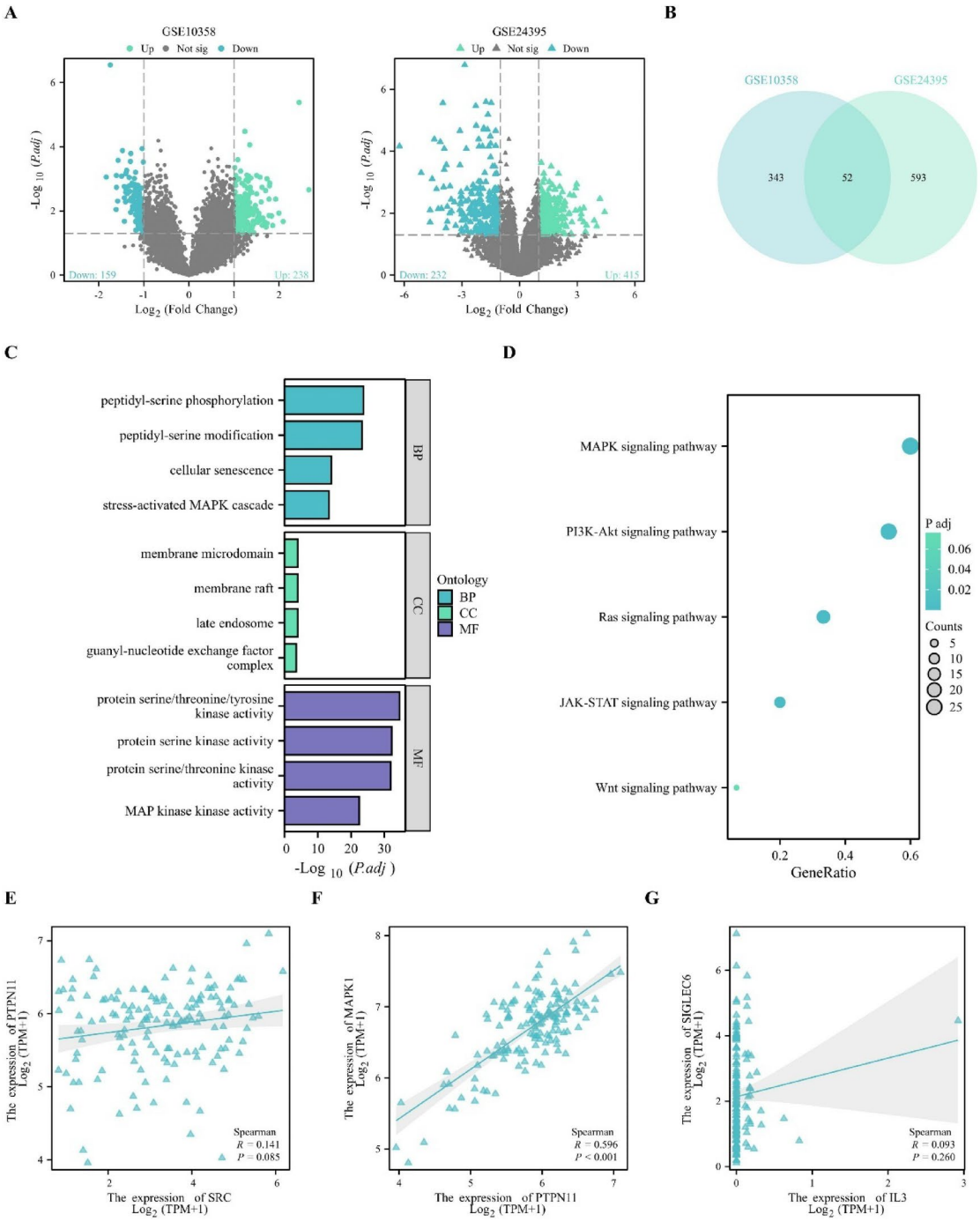

Fig. 1. Bioinformatics Analysis of AML. (**A**) Volcano plots of differential genes in the GSE10358 and GSE24395 datasets; (**B**) Venn diagram of differential genes; (**C**) Bar chart of GO enrichment analysis; (**D**) Bubble chart of KEGG enrichment analysis; (**E**) Scatter plot of the correlation between Src and SHP2 (PTPN11); (**F**) Scatter plot of the correlation between SHP2 (PTPN11) and ERK1/2 (MAPK1); (**G**) Scatter plot of the correlation between IL-3 and Siglec6.

the oe-Siglec6 + Dasatinib + Lovastatin + IL-3 monoclonal antibody group showed decreased expression levels of MMP2, MMP9, CyclinA1, CyclinD1 and Ki-67 proteins, cell migration ability, and cell activity (Fig. 4A-D). This demonstrates that Siglec6 promotes the proliferation and invasion-metastasis abilities of AML through the SHP2/Src/ERK/IL-3 axis.

5. In Vitro and In Vivo Experiments Demonstrate that Siglec6 CAR-T Inhibits the Progression of AML.

MOLM-13 cells were co-cultured with CAR-T cells and divided into five groups: oe-NC, oe-NC + CAR-T, oe-Siglec6, oe-Siglec6 + CAR-T, and oe-Siglec6 + Siglec6 CAR-T. Firstly, the results of Western blot experiments showed that the expression levels of cleaved-Caspase-3 and cleaved-Caspase-9 were significantly higher in the

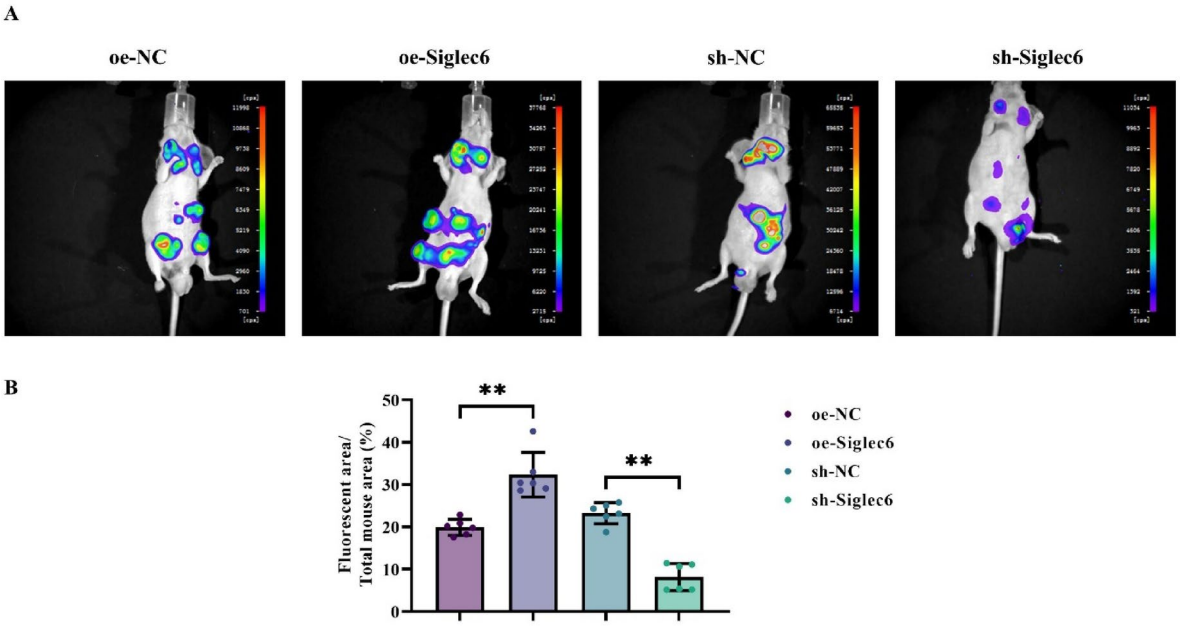

Fig. 2. In Vivo Experiments Demonstrate that High Expression of Siglec-6 Promotes the Distribution and Content Level of AML. (**A**) In vivo imaging technology detects the tumor formation of AML after treatment with oe-NC, oe-Siglec6, sh-NC, sh-Siglec6 in mice; (**B**) Statistical analysis of in vivo imaging technology detecting the tumor formation of AML after treatment with oe-NC, oe-Siglec6, sh-NC, sh-Siglec6 in mice. Data are expressed as mean ± standard deviation. $N = 6$; $^{**}P < 0.01$.

oe-NC + CAR-T group compared to the oe-NC group, while the expression levels of cleaved-Caspase-3 and cleaved-Caspase-9 in the oe-Siglec6 group showed no significant changes. Caspase-9 expression levels did not change significantly. The expression levels of cleaved-Caspase-3 and cleaved-Caspase-9 were significantly elevated in the oe-Siglec6 + CAR-T group compared to the oe-Siglec6 group. The expression levels of cleaved-Caspase-3 and cleaved-Caspase-9 were further increased in the oe-Siglec6 + Siglec6 CAR-T group compared to the oe-Siglec6 + CAR-T group (Fig. 5A). Apoptosis levels of AML cells were detected by flow cytometry. It was found that compared with the oe-NC group, the oe-NC + CAR-T group showed increased apoptosis levels of AML cells, while the oe-Siglec6 group showed no significant change in apoptosis levels. Compared with the oe-Siglec6 group, the oe-Siglec6 + CAR-T group showed increased apoptosis levels of AML cells. Compared with the oe-Siglec6 + CAR-T group, the oe-Siglec6 + Siglec6 CAR-T group showed further increased apoptosis levels of AML cells (Fig. 5B). In vivo experiments were conducted using NOD/SCID mice. MOLM-13 cells coupled with luciferase were injected into mice, and CAR-T treatment was administered, also divided into five groups: oe-NC, oe-NC + CAR-T, oe-Siglec6, oe-Siglec6 + CAR-T, and oe-Siglec6 + Siglec6 CAR-T. In vivo imaging detected the distribution of AML and found that compared with the oe-NC group, the oe-NC + CAR-T group showed weakened distribution of AML. The oe-Siglec6 group showed no significant change in AML distribution. Compared with the oe-Siglec6 group, the oe-Siglec6 + CAR-T group showed weakened distribution of AML cells. Compared with the oe-Siglec6 + CAR-T group, the oe-Siglec6 + Siglec6 CAR-T group showed further weakened distribution of AML cells (Fig. 5C). The above results suggested that Siglec6 CAR-T could target Siglec6 on AML and act on SHP2/Src/IL-3/ERK axis to inhibit tumor progression (Fig. 6).

Discussion

AML is a heterogeneous disease with diverse genomic alterations and mutations. Significant therapeutic advancements have been made through large-scale genomic assessments, providing detailed insights into AML's molecular structure[13]. However, primary resistance and disease relapse remain major challenges, affecting more than half of AML patients due to diverse clones and somatic heterogeneity. CAR-T therapy, targeting antigens like CD33, CD123, CLL-1, and NKG2DLs, shows promise but faces issues such as poor persistence, insufficient efficacy, and target escape[14]. Therefore, finding new CAR-T targets is a top priority. Siglec-6 is an immunoglobulin-like lectin that belongs to the CD33-related subgroup of Siglecs and is mainly expressed in the placenta, mast cells, and memory B cells[15]. It is also highly expressed in AML. Interestingly, Siglec-6 is normally expressed in normal myeloid cells, suggesting that Siglec-6 may play an important role in the diagnosis and treatment of AML and has the potential to be a potential target for CAR-T. Therefore, we have explored the feasibility of Siglec6 as an AML target and its molecular mechanisms in depth.

We first intervened with Siglec6 in AML through lentiviral infection and selected NOD/SCID mice to explore the relationship between the expression level of Siglec6 in AML and the progression of AML through in vivo imaging. After treating the AML, we injected it into the mice through the tail vein and found that after overexpressing Siglec6 in AML, the tumor's proliferative ability and distribution level in the body were

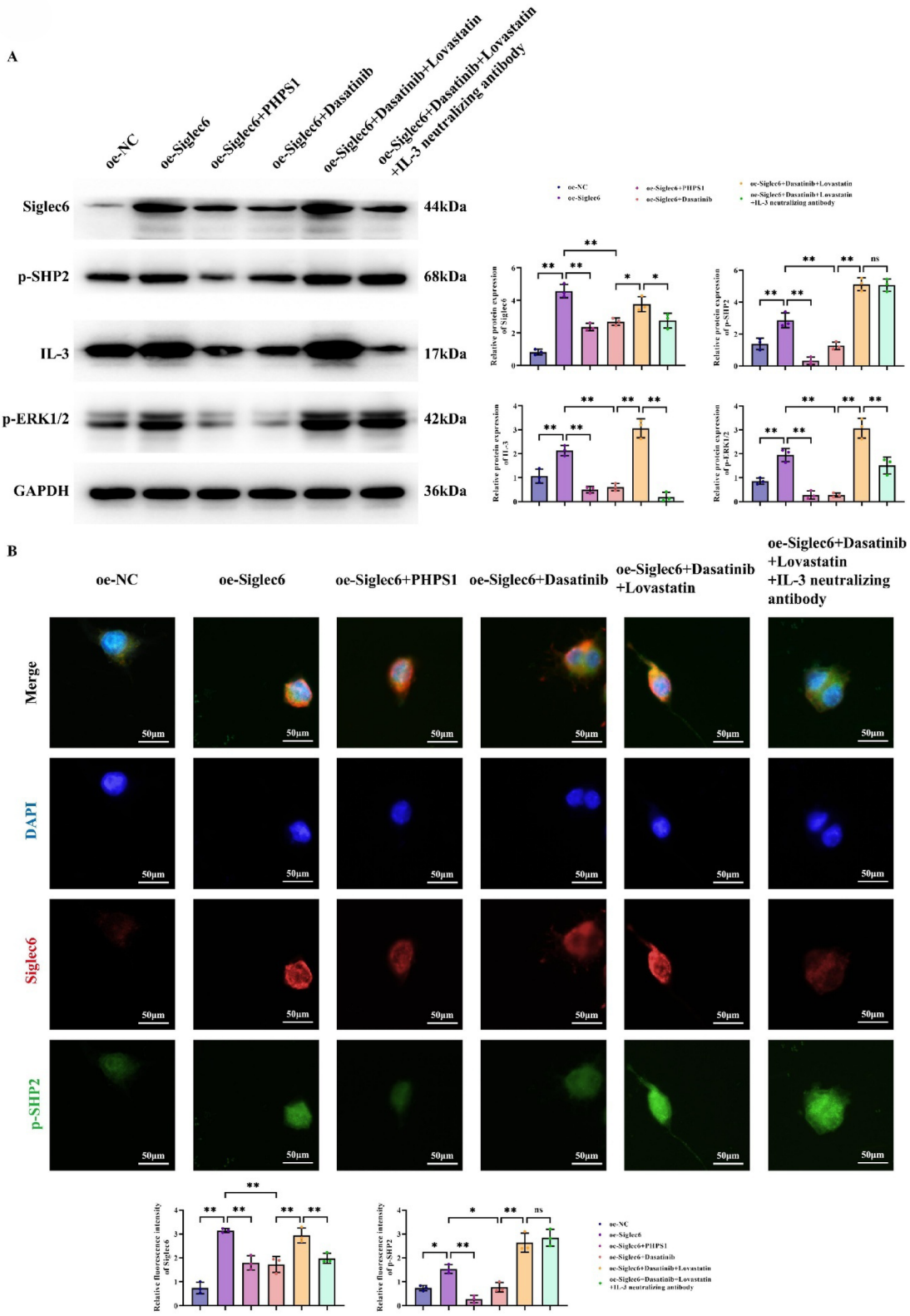

Fig. 3. Siglec6 Acts on AML through the SHP2/Src/ERK/IL-3 Axis. (**A**) Western blot detects the protein expression levels of Siglec6, p-SHP2, IL-3, pERK1/2 in AML cells in the oe-NC, oe-Siglec6, oe-Siglec6 + PHPS1, oe-Siglec6 + Dasatinib, oe-Siglec6 + Dasatinib + Lovastatin, and oe-Siglec6 + Dasatinib + Lovastatin + IL-3 monoclonal antibody groups; GAPDH as control protein; (**B**) Immunofluorescence detects the protein expression levels of Siglec6 and p-SHP2 in the oe-NC, oe-Siglec6, oe-Siglec6 + PHPS1, oe-Siglec6 + Dasatinib, oe-Siglec6 + Dasatinib + Lovastatin, and oe-Siglec6 + Dasatinib + Lovastatin + IL-3 monoclonal antibody groups. Data are expressed as mean ± standard deviation. $N = 3$; $^{*}P < 0.05$; $^{**}P < 0.01$; $^{ns}P > 0.05$.

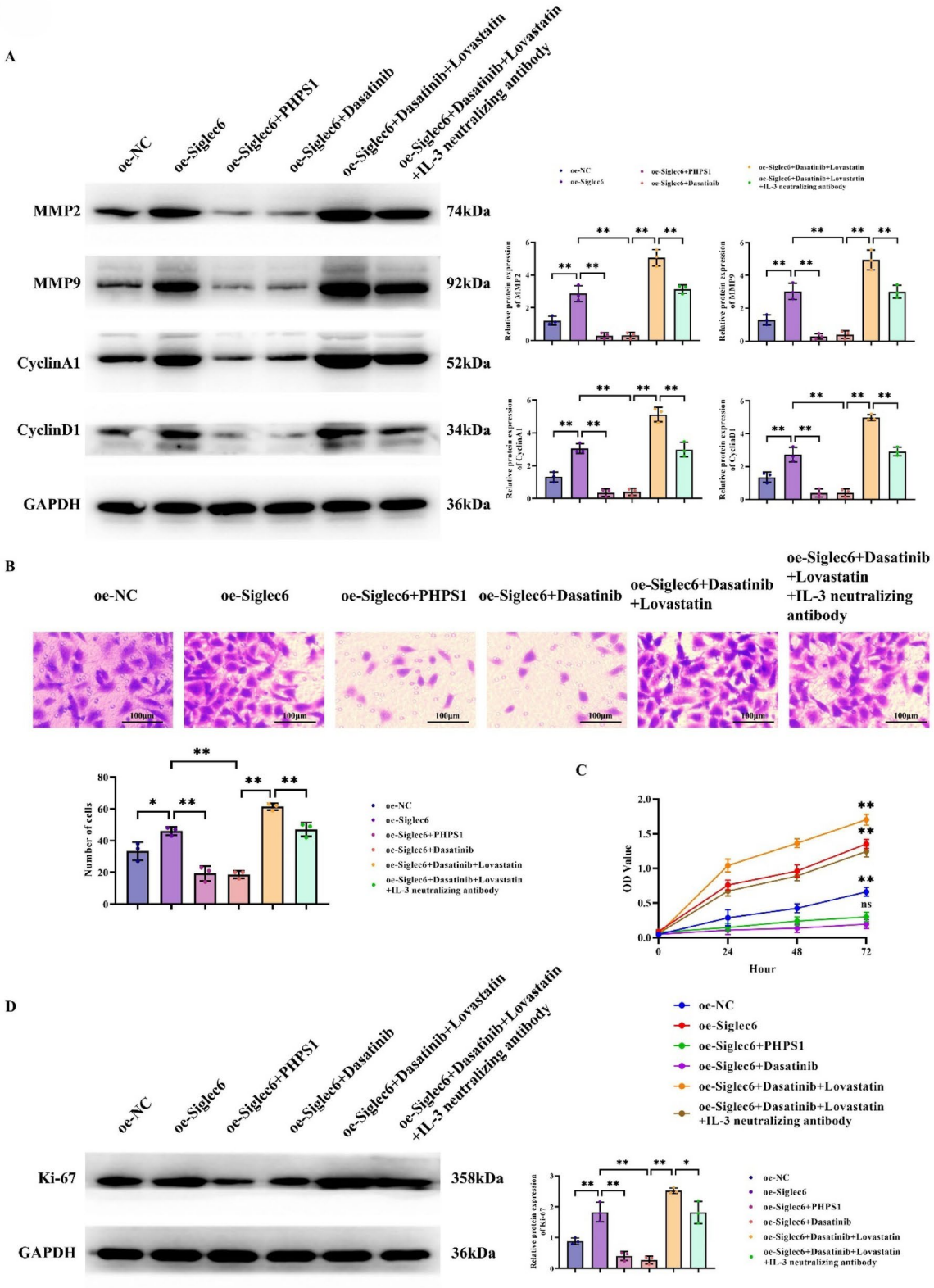

enhanced; whereas after knocking down Siglec6, the phenomenon was reversed, and the tumor distribution in the body was weakened, proving the importance of Siglec6 expression levels in the progression of AML. Next, we explored how Siglec6 promotes the progression of AML. Siglec6 is a transmembrane receptor that is specifically expressed on AML, and its cytoplasmic tail contains an ITIM and an ITIM-like motif, which have signal transduction functions. It can be phosphorylated by Src family kinases, thereby recruiting SH-2 domain-containing phosphatase SHP2, providing a molecular platform[16]. SHP2, full name Src homology 2 domain-containing protein tyrosine phosphatase, is a non-receptor type protein tyrosine phosphatase encoded by the *PTPN11* gene. SHP2 plays an important role in cellular signal transduction, especially in the invasion,

◀**Fig. 4**. Siglec6 Promotes the Proliferation and Invasion-Metastasis Abilities of AML through the SHP2/Src/ERK/IL-3 Axis. (**A**) Western blot detects the expression levels of MMP2, MMP9, CyclinA1, CyclinD1 proteins in AML cells in the oe-NC, oe-Siglec6, oe-Siglec6 + PHPS1, oe-Siglec6 + Dasatinib, oe-Siglec6 + Dasatinib + Lovastatin, and oe-Siglec6 + Dasatinib + Lovastatin + IL-3 monoclonal antibody groups; (**B**) Transwell assay detects the invasion ability of AML cells in the oe-NC, oe-Siglec6, oe-Siglec6 + PHPS1, oe-Siglec6 + Dasatinib, oe-Siglec6 + Dasatinib + Lovastatin, and oe-Siglec6 + Dasatinib + Lovastatin + IL-3 monoclonal antibody groups; (**C**) CCK8 assay detects the proliferation ability of AML cells in the oe-NC, oe-Siglec6, oe-Siglec6 + PHPS1, oe-Siglec6 + Dasatinib, oe-Siglec6 + Dasatinib + Lovastatin, and oe-Siglec6 + Dasatinib + Lovastatin + IL-3 monoclonal antibody groups; (**D**) Western blot detects the expression levels of Ki-67 in AML cells in the oe-NC, oe-Siglec6, oe-Siglec6 + PHPS1, oe-Siglec6 + Dasatinib, oe-Siglec6 + Dasatinib + Lovastatin, and oe-Siglec6 + Dasatinib + Lovastatin + IL-3 monoclonal antibody groups; GAPDH as control protein; Data are expressed as mean ± standard deviation. $N = 3$; $^{*}P < 0.05$; $^{**}P < 0.01$; $^{ns}P > 0.05$.

metastasis, proliferation, apoptosis, and drug resistance of tumor cells. When SHP2 is activated, it promotes the phosphorylation of ERK[17]. ERK, full name extracellular signal-regulated kinase, is a member of the Mitogen-Activated Protein Kinases (MAPKs) family and is mainly involved in regulating key biological processes such as cell proliferation, differentiation, survival, and apoptosis[18]. When ERK is activated, it promotes the invasive migration and proliferation capabilities of tumors. At the same time, the overactivation of SHP2 protein also promotes the expression of IL-3 [19]. IL-3, full name multi-colony stimulating factor, can act as a hematopoietic growth factor and activate cytokines, and its increased levels will promote the protein expression level of Siglec6, forming a positive feedback loop, further promoting the invasive migration and proliferation capabilities of AML[20]. Based on this, we set up in vitro experiments and chose MOLM-13 cells for analysis. We set up rescue experiments, dividing the cells into six groups: oe-NC, oe-Siglec6, oe-Siglec6 + PHPS1, oe-Siglec6 + Dasatinib, oe-Siglec6 + Dasatinib + Lovastatin, and oe-Siglec6 + Dasatinib + Lovastatin + IL-3 neutralizing antibody. We detected the protein expression levels of Siglec6, p-SHP2, IL-3, pERK1/2, proliferation-related proteins CyclinA1, CyclinD1, and invasion-related proteins MMP2 and MMP9 by Western blot. We found that compared with the oe-NC group, after overexpressing Siglec6, the protein expression levels of Siglec6, p-SHP2, IL-3, pERK1/2, CyclinA1, CyclinD1, MMP2, and MMP9 increased, and the corresponding use of Src inhibitors, SHP2 agonists, and IL-3 neutralizing antibodies reversed the protein expression levels. Transwell and CCK8 experiments also proved this point. It indicates that in AML, Siglec6 promotes the proliferation, invasion, and migration capabilities of AML through the SHP2/Src/ERK/IL-3 axis.

Based on the previous research, we found that Siglec6 can affect the progression of AML through a series of molecular pathways, suggesting that Siglec6 can be a potential target for CAR-T. In this part, we focus on whether Siglec6 can be an effective target for CAR-T therapy. We modified T cells to target Siglec6 on AML. We co-cultured ordinary CD19 CAR-T, Siglec6 CAR-T with AML and detected the apoptosis level of AML cells by flow cytometry. We found that MOLM-13 cells cultured with Siglec6 CAR-T had stronger apoptosis capabilities. Further in vivo experiments were conducted by injecting MOLM-13 cells into NOD/SCID mice and treating the mice with CAR-T. In vivo imaging technology detected the distribution and content of tumors in the mice. We observed a significant phenomenon: the number of tumors in mice treated with Siglec6 CAR-T was significantly less than those treated with CD19 CAR-T. This result indicates that Siglec6 CAR-T therapy may be more effective than CD19 CAR-T therapy in inhibiting tumor growth and reducing the number of tumors. For the occurrence of this phenomenon, we speculate that it may be due to the activated Siglec6 CAR-T cells producing interferons that directly attack tumor cells, leading to tumor cell death[21]. In related studies, it has been confirmed that CAR-T cells can kill tumor cells by releasing interferons and other cytokines[22]. Therefore, Siglec6 CAR-T cells may produce the killing effect on AML tumor cells by producing interferons and other cytokine.

In summary, we have demonstrated that Siglec6 CAR-T can target Siglec6 on AML and act on the SHP2/Src/IL-3/ERK axis to inhibit tumor progression. The discovery of this mechanism provides a molecular explanation for how Siglec6 CAR-T cells exert therapeutic effects on AML and offers potential intervention points for future treatment strategies. However, it is regrettable that we have not validated the mechanism of action of Siglec6 CAR-T at the clinical level. This limitation prompts us to further conduct clinical trials to evaluate the efficacy and safety of Siglec6 CAR-T cell therapy in actual patients, thereby providing more precise and effective treatment options for AML patients.

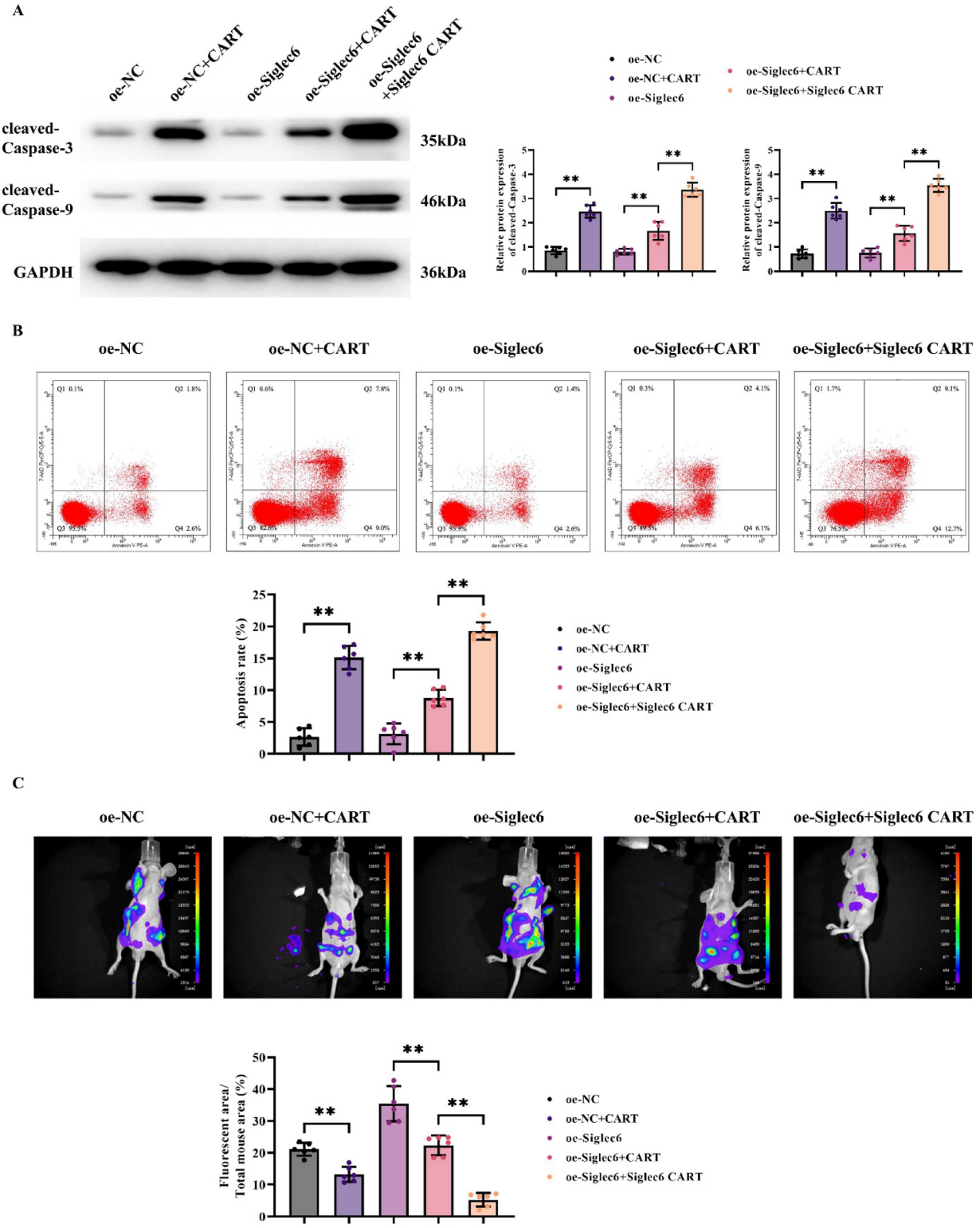

Fig. 5. In Vitro and In Vivo Experiments Demonstrate that Siglec6 CAR-T Inhibits the Progression of AML. (**A**) Western blot detects the expression levels of cleaved-Capase-3 and cleaved-Capase-9 in AML cells in the oe-NC, oe-NC + CAR-T, oe-Siglec6, oe-Siglec6 + CAR-T, and oe-Siglec6 + Siglec6 CAR-T groups after co-culturing with CAR-T cells; GAPDH as control protein; (**B**) Flow cytometry detects the apoptosis levels of MOLM-13 cells in the oe-NC, oe-NC + CAR-T, oe-Siglec6, oe-Siglec6 + CAR-T, and oe-Siglec6 + Siglec6 CAR-T groups after co-culturing with CAR-T cells; C: In vivo experiments detect the distribution of MOLM-13 cells in the oe-NC, oe-NC + CAR-T, oe-Siglec6, oe-Siglec6 + CAR-T, and oe-Siglec6 + Siglec6 CAR-T groups. Data are expressed as mean ± standard deviation. $N = 3$; $^{*}P < 0.05$; $^{**}P < 0.01$; $^{ns}P > 0.05$.

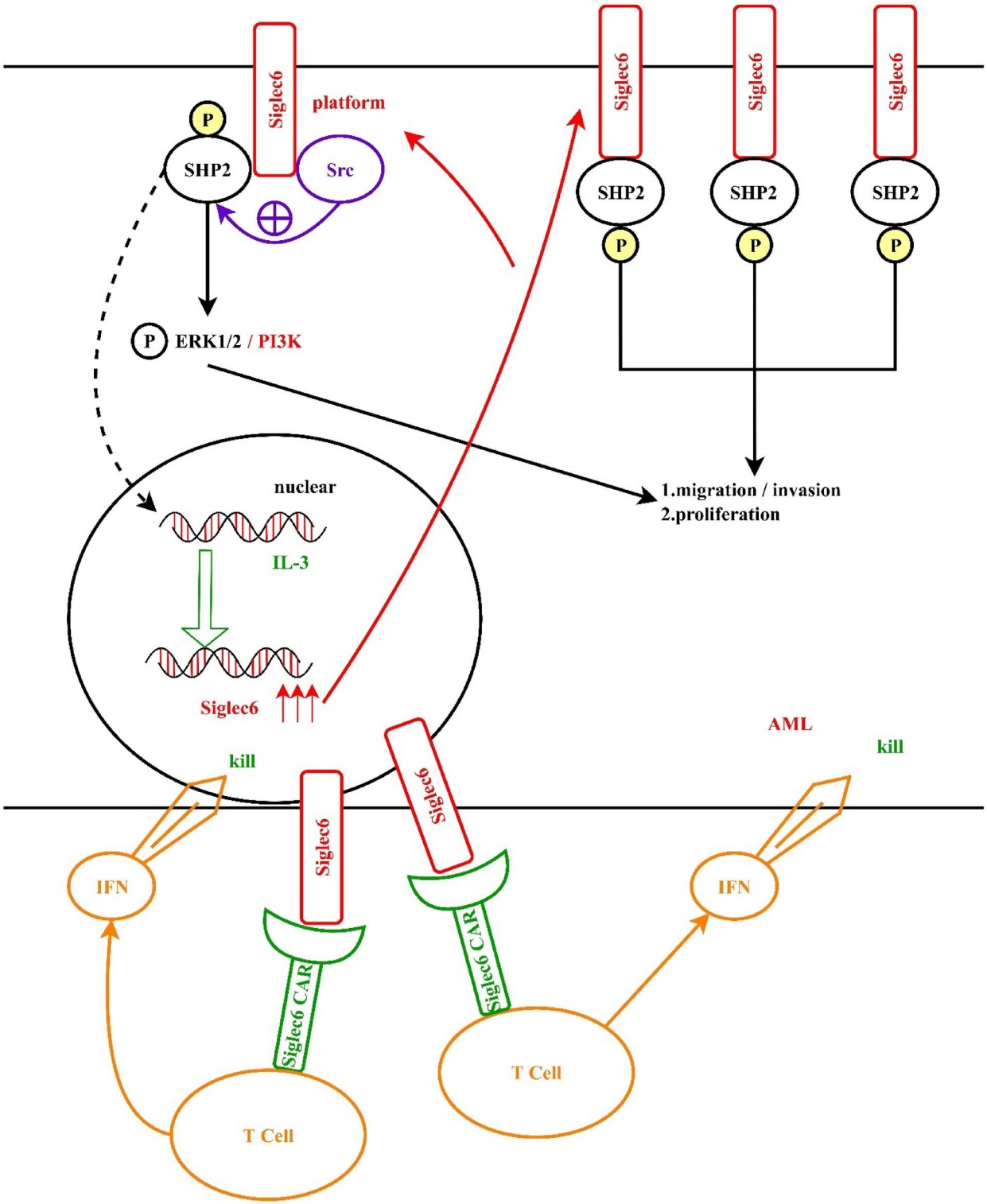

Fig. 6. Siglec6 CAR T cells suppressed progression of AML via inhibiting Siglec6/ SHP2/ Src/ IL-3/ ERK signaling.

Data availability

The datasets generated during and/or analysed during the current study are available from the corresponding author on reasonable request.

Received: 3 November 2024; Accepted: 28 April 2025
Published online: 28 May 2025

References

1. Dinardo, C. D. & Wei, A. H. How I treat acute myeloid leukemia in the era of new drugs [J]. *Blood* **135** (2), 85–96 (2020).
2. Shimony, S., Stahl, M. & Stone, R. M. Acute myeloid leukemia: 2023 update on diagnosis, risk-stratification, and management [J]. *Am. J. Hematol.* **98** (3), 502–526 (2023).
3. Kayser, S. & Levis, M. J. The clinical impact of the molecular landscape of acute myeloid leukemia [J]. *Haematologica* **108** (2), 308–320 (2023).
4. Jin, X. et al. CAR-T cells dual-target CD123 and NKG2DLs to eradicate AML cells and selectively target immunosuppressive cells [J]. *Oncoimmunology* **12** (1), 2248826 (2023).
5. Carter, J. L. et al. Targeting multiple signaling pathways: the new approach to acute myeloid leukemia therapy [J]. *Signal. Transduct. Target. Therapy.* **5** (1), 288 (2020).
6. Liu, Y. et al. Development of mRNA lipid nanoparticles: targeting and therapeutic aspects [J]. *Int. J. Mol. Sci.*, **25**(18). (2024).
7. Lou, H. & Cao, X. Antibody variable region engineering for improving cancer immunotherapy [J]. *Cancer Commun. (London England).* **42** (9), 804–827 (2022).
8. Jia, Y. et al. Upregulation of Siglec-6 induces mitochondrial dysfunction by promoting GPR20 expression in early-onset preeclampsia [J]. *J. Translational Med.* **22** (1), 674 (2024).
9. Griciuc, A. & Tanzi, R. E. The role of innate immune genes in Alzheimer's disease [J]. *Curr. Opin. Neurol.* **34** (2), 228–236 (2021).
10. Urs, A. P., Goda, C. & Kulkarni, R. Remodeling of the bone marrow microenvironment during acute myeloid leukemia progression [J]. *Annals Translational Med.* **12** (4), 63 (2024).
11. Meng, S. et al. Revealing neuropilin expression patterns in pancreatic cancer: from single–cell to therapeutic opportunities (Review) [J]. *Oncol. Lett.* **27** (3), 113 (2024).
12. Hou, Y. et al. How a single mutation alters the protein structure: a simulation investigation on protein tyrosine phosphatase SHP2 [J]. *RSC Adv.* **13** (7), 4263–4274 (2023).
13. Stubbins, R. J. et al. Management of acute myeloid leukemia: A review for general practitioners in oncology [J]. *Curr. Oncol. (Toronto Ont).* **29** (9), 6245–6259 (2022).
14. Yu, J. et al. *Clinical Implications of Recurrent Gene Mutations in Acute Myeloid Leukemia [J]*94 (Experimental hematology & oncology, 2020).
15. Nunes, J. et al. Siglec-6 as a therapeutic target for cell migration and adhesion in chronic lymphocytic leukemia [J]. *Nat. Commun.* **15** (1), 5180 (2024).
16. Stefanski, A. L. et al. Siglec-6 signaling uses Src kinase tyrosine phosphorylation and SHP-2 recruitment [J]. *Cells*, **11**(21). (2022).
17. Tang, K. H. et al. Combined Inhibition of SHP2 and CXCR1/2 promotes antitumor T-cell response in NSCLC [J]. *Cancer Discov.* **12** (1), 47–61 (2022).
18. Shi, Y. et al. Remimazolam protects the liver from ischemia-reperfusion injury by inhibiting the MAPK/ERK pathway [J]. *BMC Anesthesiol.* **24** (1), 251 (2024).
19. Richards, C. E. et al. Protein tyrosine phosphatase Non-Receptor 11 (PTPN11/Shp2) as a driver oncogene and a novel therapeutic target in Non-Small cell lung Cancer (NSCLC) [J]. *Int. J. Mol. Sci.* **24**(13), 10545 (2023).
20. Bilousova, G. et al. Impaired DNA replication within progenitor cell pools promotes leukemogenesis [J]. *PLoS Biol.* **3** (12), e401 (2005).
21. Zheng, W. et al. Inhalable CART cell-derived exosomes as Paclitaxel carriers for treating lung cancer [J]. *J. Translational Med.* **21** (1), 383 (2023).
22. Gruenbach, M. et al. cART restores transient responsiveness to IFN type 1 in HIV-Infected humanized mice [J]. *J. Virol.* **96** (21), e0082722 (2022).

Acknowledgements

None.

Author contributions

This study was conceived and conceptualized by Y.F.W. and H.F.Z. Experiments were designed performed and analyzed by Q.L., L.L., S.G., Z.Z., J.M., S.L., Z.C., and L.C. did data interpretation and original draft preparation. Y.F.W. and H.F.Z. reviewed, edited, and approved the final draft. All authors have read and agreed to the published version of the manuscript.

Funding sources

National Natural Science Foundation of China (82270208, YF, Wang), Tianjin Medical University Cancer Institute and Hospital "The 14th Five-Year" Summit Subject Support Plan (7-2-12-1, YF Wang).

Declarations

Competing interests

The authors declare no competing interests.

Ethics approval

The study was approved by the Ethics Committee of Tianjin Jinke Bona Biotechnology Co. The ethical number is 20230039.

Additional information

Supplementary Information The online version contains supplementary material available at https://doi.org/10.1038/s41598-025-00456-x.

Correspondence and requests for materials should be addressed to H.Z. or Y.W.